GEOPHYSICAL RESEARCH LETTERS, VOL. 34, L05817, doi:10.1029/2006GL029161, 2007



# Potential for attenuation-based estimations of rainfall rate from CloudSat

Sergey Y. Matrosov[1]

Received 20 December 2006; revised 27 January 2007; accepted 7 February 2007; published 13 March 2007.

[1] Attenuation of radar signals in rain increases with frequency while the variability of non-attenuated reflectivity of rainfall diminishes as resonance scattering effects become more pronounced at higher radar frequencies. At mm-wavelength frequencies, attenuation often becomes the dominant factor responsible for apparent reflectivity changes in vertical. This study presents an attenuation-based method to retrieve vertical profiles of rain rate from nadir-pointing W-band (94 GHz) radars. The quantitative assessments of retrieval errors are discussed, and an illustration of the retrievals using measurements from the spaceborne 94 GHz CloudSat radar is shown. As a consistency check, the spaceborne W-band radar retrievals are compared with concurrent estimates from a ground-based weather surveillance radar. **Citation:** Matrosov, S. Y. (2007), Potential for attenuation-based estimations of rainfall rate from CloudSat, *Geophys. Res. Lett.*, *34*, L05817, doi:10.1029/2006GL029161.

## 1. Introduction

[2] The world's first satellite-borne W-band (94 GHz) nadir-pointing cloud radar (CloudSat) has been successfully collecting data since June 2006. Though the main objective of this radar is to acquire global information on clouds, it also resolves many precipitation systems, and it has been suggested previously that the CloudSat data can be used to retrieve light rainfall parameters [e.g., *L'Ecuyer and Stephens*, 2002; *Stephens and the CloudSat Science Team*, 2002].

[3] The traditional non-polarimeric radar approaches for rainfall retrievals are based on relating the equivalent radar reflectivity factor, $Z_e$, (hereafter "reflectivity") to rain rate, $R$. Attenuation of radar signals in rain has been almost always considered as a factor that impedes rain retrievals. Special techniques have been developed to remove the effects of attenuation when they become significant. One example is the Hitschfeld-Borden scheme [*Hitschfeld and Bordan*, 1954], which was used for the Tropical Rainfall Measuring Mission's (TRMM) satellite-borne $K_u$-band (13.8 GHz) radar [e.g., *Iguchi et al.*, 2000]. After correcting attenuation effects, estimates of non-attenuated reflectivity are related to rain rate by using $Z_e - R$ relations.

[4] While at cm-wavelengths, attenuation corrections are relatively modest for most rains, at mm-wavelengths such as those at $K_a$-band ($\sim$35 GHz) and especially W-band, attenuation is strong and it often becomes a dominant factor responsible for systematic reflectivity differences with respect to the value that would be observed in absence of raindrops between a given sampling volume and the radar. In the attenuation-based radar approach for retrieving rain rates, changes of measured reflectivity caused by attenuation are the useful signal while the vertical variability in non-attenuated reflectivity is a factor that contributes to retrieval uncertainty.

[5] The attenuation-based rainfall profiling method was first applied to $K_a$-band ground- based vertically pointing radar data. At $K_a$-band, the attenuation coefficient in rain, $\alpha$, is proportional to $R$, and the proportionality coefficient exhibits very little variability due to drop size distributions (DSD) details and temperature [*Matrosov*, 2005]. Given this proportionality, the rainfall rate, $R$, is estimated by means of the range derivative of the measured (i.e., attenuated) reflectivity. It was demonstrated that for the effective resolution interval of 1 km, the attenuation-based method at $K_a$-band provides good results for stratiform and convective rains that have $R > 4$ mm h$^{-1}$ and which do not exhibit strong slanted patterns of measured reflectivity [*Matrosov et al.*, 2006].

## 2. Formulation of the Method for CloudSat

[6] For 94 GHz, Figure 1 shows the attenuation - rain rate and non-attenuated reflectivity–rain rate scatter plots (for $R > 1$ mm h$^{-1}$) as calculated using the T-matrix method from experimental DSDs collected during the Wallops Island, Virginia (2001) and Miami, Florida (2002) field projects. It can be seen from Figure 1 that there is a strong correlation between $\alpha$ and $R$. At the same time, except for a few data points that constitute less than 1% of the total number of experimental DSDs considered here, values of non-attenuated reflectivity at W-band do not exceed the level of about 26 dBZ. This is a result of the fact, that for larger drops, backscattering efficiency oscillates with changing drop size. The variability in non-attenuated reflectivities generally diminishes as $R$ increases.

[7] The attenuation-based rainfall retrieval method requires proportionality between $\alpha$ and $R$. While this condition is practically satisfied for $K_a$-band, at W-band the best fit power-law $R - \alpha$ relation is slightly non-linear (the solid curve in Figure 1), and it also exhibits more significant data scatter. The linear model for the $R - \alpha$ relation at 94 GHz needs to be used to apply the attenuation-based method. This model (the dashed line in Figure 1) was derived in such a way that it provides a zero intercept and enforces a zero mean bias for the $R - \alpha$ relation:

$$R\left(\text{mm h}^{-1}\right) = k(h)\beta\alpha\left(\text{dB km}^{-1}\right) \quad (1)$$

[1]Cooperative Institute for Research in Environmental Sciences, University of Colorado and NOAA Earth Systems Research Laboratory, Boulder, Colorado, USA.


0094-8276/07/2006GL029161$05.00

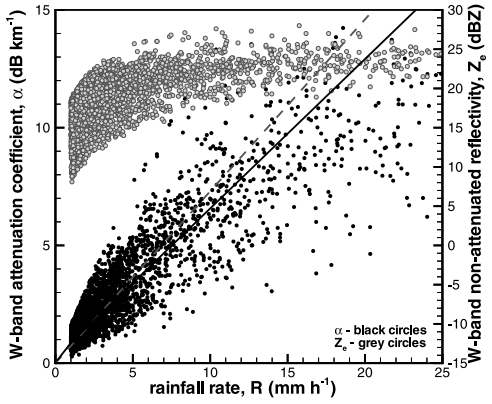


**Figure 1.** $R - \alpha$ (solid circles) and non-attenuated $Z_e - R$ (grey circles) scatter-plots at W-band for $t$ = 5°C. Lines represent the best fit power $R = 1.17\ \alpha^{1.09}$ (solid) and linear $R = 1.24\ \alpha$ (dashed) models for the $R - \alpha$ relations (using $\alpha$ as an independent variable).

[8] It can also be seen from Figure 1 that while there is a strong and almost linear relation between $R$ and $\alpha$, there is little correlation between $R$ (and, hence $\alpha$) and absolute values of $Z_e$. This is especially true for $R > 4–5$ mm h$^{-1}$ when $Z_e$ varies in a relatively narrow interval. This fact indicates that the radar approaches which use absolute values of $Z_e$ (measured or corrected for attenuation) in $R - Z_e$ and/or $\alpha - Z_e$ relations have a very limited use at W-band.

[9] In equation (1) $k(h)$ accounts for the changes of air density $\rho_a$ with height above sea level, $h$:

$$k(h) \approx 1.1\rho_a(\mathrm{h})^{-0.45}, \rho_a \text{ in kg m}^{-3} \quad (2)$$

Modeling $R - \alpha$ relations with experimental DSD sets from other projects (including ones held in California and Colorado) indicates (not shown) that the non-linearity of these relations remains rather modest with the exponents of the best-fit power laws varying in an approximate range from 0.94 to 1.16. The linear $R - \alpha$ model for different DSD sets yields the best fit proportionality coefficient $\beta$ in (1) varying in a range between about 1 and 1.4. The relative standard deviation (RSD) of the data points in $R - \alpha$ scatter plots for an individual DSD set around the best fit proportionality relation is about 35%. The mean value of $\beta = 1.2$ was further used in this study. The uncertainty of the $\beta$ coefficient can be assumed to be about ±16% thus covering the range 1–1.4. Assuming the independence of error contributions due to $\beta$ (∼16%) and due to data scatter around the best fit proportionality relation (∼35%), an RSD uncertainty of relating $R$ from $\alpha$ using (1) can be estimated as about 38% ($0.38^2 \approx 0.35^2 + 0.16^2$).

[10] The attenuation coefficient $\alpha$ is estimated by means of the half (due to a two-way propagation) of the mean height derivate of the measured (i.e., attenuated) reflectivity, $Z_{em}$, at the effective height resolution interval:

$$\alpha(h) = 0.5 \cdot [\partial Z_{em}(h)/\partial h] - G(h) \quad (3)$$

The gaseous ($O_2$ and $H_2O$) attenuation correction term $G(h)$ is determined by the absolute humidity, pressure and temperature [*Matrosov et al.*, 2004]. The temperature is calculated assuming the mean gradient of −6.5°C below the freezing level which is approximated by the reflectivity bright band (i.e., the zone of enhanced reflectivity due to melting ice particles). The standard pressure height distribution is assumed, and the absolute humidity is calculated using the temperature information and assuming 95% relative humidity in the rain layer.

[11] The derivative $\partial Z_{em}(h)/\partial h$ is calculated as a mean slope of the $Z_{em}(h)$ dependence at the five CloudSat resolution bins spaced by 0.24 km apart using the least mean square (LMS) method. As a result, the effective spatial resolution of the method is ∼1.2 km, while, due to the "sliding window" approach, the rain rate estimates are obtained at each resolution bin within the rain layer, excluding 0.6 km below the freezing level and 0.6 km above the ground to avoid possible contamination by the melting layer and ground returns. Note that the actual resolution of the CloudSat radar data is about 0.48 km, and the data are oversampled by about a factor of 2, thus providing the apparent resolution of 0.24 km.

## 3. Approximate Estimates of Retrieval Errors

[12] The uncertainty of the mean relation (1) and the vertical variability of non-attenuated reflectivities, $Z_e$, are the two main contributors to rain rate retrieval errors. While at $K_a$-band, the latter contributor is usually prevalent, at W-band the relative strength of the former is often higher, especially for $R > 5$ mm h$^{-1}$. Figure 2 depicts the reflectivity range $\Delta_Z$ (curve a) as a function of rain rate $R_0$ defined in such a way that 68% of all DSDs considered in Figure 1 with $R > R_0$ (i.e., ± the standard deviation range, assuming the Gaussian distribution) have non-attenuated reflectivity values in a range between 26 dBZ and (26 − $\Delta_Z$)dBZ. In other words, the value of $\Delta_Z$ ($R_0$) represents for $R > R_0$ a standard deviation of possible changes in non-attenuated $Z_e$ which contribute to the retrieval uncertainty.

[13] Figure 2 also shows (curve b) estimates of retrieval errors assuming the independence of the two main error contributions due to the above estimated 38% uncertainty in relating rain rate from attenuation and also due to the variability in non-attenuated reflectivity at a $\Delta_h$ = 1.2 km interval used for estimating the height derivate. Assuming

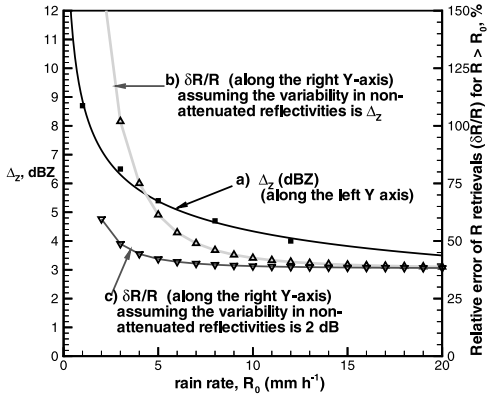


**Figure 2.** The reflectivity range $\Delta_Z$ (curve a) and the uncertainty of retrievals as a function of rain rate (curve b).

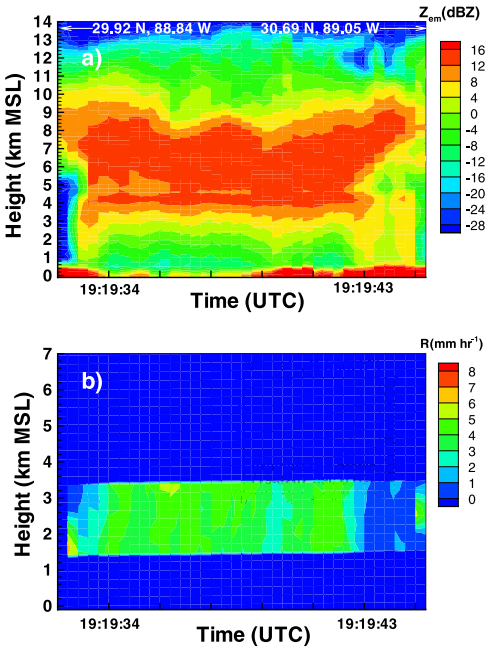


**Figure 3.** (a) Time-height cross-sections of the CloudSat measurements and (b) rain rate estimates for 7/31/06. Note a vertical scale change in Figure 3b to provide better details.

normal atmospheric conditions, these error estimates were performed using the equation:

$$(\delta R/R)^2 = 0.38^2 + \left[\Delta_Z/\left(2\beta^{-1}\Delta_h R\right)\right]^2 \qquad (4)$$

The second term in (4) reflects an upper bound error due to the variability of non-attenuated reflectivities which (at worst) can be as large as $\Delta_Z$ (in a standard deviation sense) However, in most practical cases this variability will be less than $\Delta_Z$, especially at the retrieval resolution interval of 1.2 km. Curve c in Figure 2 shows estimates of $\delta R/R$ when a 2 dB variability in non-attenuated reflectivities (which is typical for convective rains at about 1 km vertical range) was used instead of $\Delta_Z$ in (4). For stratiform rains this variability is expected to be even smaller, thus further reducing expected errors.

[14] For lighter rain rates, error contributions due to changes of non-attenuated reflectivity can dominate. Uncertainties in accounting for gaseous attenuation are expected to result in much smaller retrieval errors compared to the two main error sources discussed above. At W-band, the temperature dependence of $\beta$ is only a few percentage points (for the range 0°C–15°C) and thus is currently neglected.

[15] The large vertical range and horizontal footprint resolutions (~0.5 km, and ~1.5 km, correspondingly) of the CloudSat radar can result in contributions from multiple scattering in measured echoes from heaver rain [*Battaglia et al.*, 2005]. It can present additional retrieval errors of the attenuation-based method since this method and practically all other radar methods assume single scattering. A detailed assessment of the multiple scattering effects in the CloudSat echoes as a function of rain rate and the layer thickness requires detailed radiation transfer modeling and justifies a separate study. It could be expected, however, that multiple scattering will affect the attenuation-based method to a somewhat lesser extent than traditional radar techniques that use absolute reflectivity estimates. This is because this method is based on gradient measurements, and thus it will be affected mainly by the differences of the multiple scattering contributions in the beginning and at the end of the interval used to estimate the height derivative of measured reflectivity. These differences will likely be smaller than the absolute values of the contributions, and, in an ideal case, could be negligible if these absolute values do not change significantly with height at the considered interval.

## 4. Illustration of the Attenuation-Based Retrievals

[16] One example of the attenuation-based rain rate retrievals from the CloudSat radar data is given below. Figure 3a shows CloudSat measurements of a precipitating system as the satellite crossed from the Gulf of Mexico onto the U.S. mainland near the Louisiana-Mississippi border on 31 July 2006. The X-axes in Figure 3 correspond approximately to an 85 km distance interval (which is also shown by the solid white line in Figure 4). The reflectivity enhancement due to ice hydrometer melting can be seen in Figure 3a just above 4 km above mean sea level (MSL). Attenuation causes a rapid decrease in measured reflectivities with range in the rain layer, but surface returns are still observed, indicating that radar signals are able to penetrate the entire rain layer. A time-height cross section of rain rate profile retrievals using the method described in section 2 is shown in Figure 3b. Note a change in the vertical scale in Figure 3b compared to Figure 3a.

[17] Figure 4 shows S-band reflectivities measured by the New Orleans's Weather Surveillance Radar-1988 Doppler (WSR-88D), which is a part of the Next Generation Weather Radar (NEXRAD) network and which has the 4- letter site identifier, KLIX. The depicted KLIX azimuthal scan corresponds to 19:19 UTC and 1.7° elevation angle. At S-band frequencies, attenuation by raindrops is very small and can be ignored for the most practical cases, so no correction to KLIX reflectivity data was introduced. The distances from the KLIX radar to the CloudSat resolution volumes in the

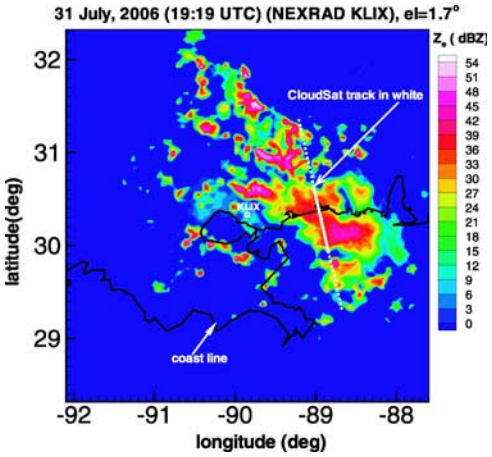


**Figure 4.** KLIX S-band radar reflectivity map.

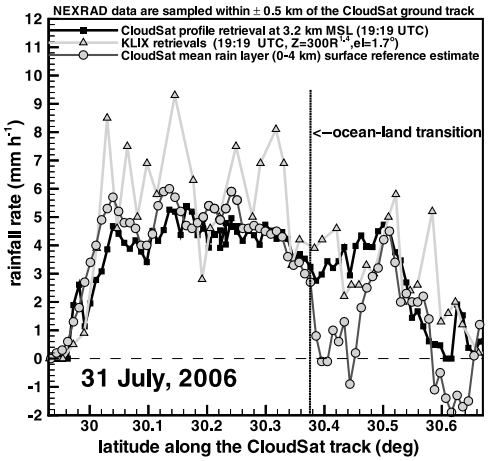


**Figure 5.** Comparisons of NEXRAD and CloudSat data.

precipitation system shown in Figure 4 were between about 83 km and 102 km.

## 5. Comparisons of NEXRAD and CloudSat Data

[18] While not being a comprehensive validation check, comparisons of KLIX and CloudSat rain rate estimates are of interest in the area of rainfall between the latitudes of 29.9° and 30.7°. The CloudSat ground track in this area is shown by the solid white line in Figure 4. Showers further south are small in size and located further than 120 km from the KLIX radar. KLIX estimates at such ranges are likely be affected by the melting layer and snow because upper parts of the KLIX beam at such distances can reach altitudes of 4 km and higher (at el = 1.7°). Figure 5 shows comparisons of rain rates retrieved from CloudSat data at an altitude of about 3.2 km MSL and estimates from the KLIX radar using the standard NEXRAD S-band relation [$Z_e$(mm$^6$ m$^{-3}$) = 300 $R^{1.4}$ (mm h$^{-1}$)].

[19] Figure 5 also shows CloudSat estimates of the mean rain rate $R_m$ in the whole rain layer $h_m$ ($h_m$ = 4.1 km) from a TRMM-like ocean reference approach [e.g., *Meneghini et al.*, 2000] when estimates are obtained assuming that a difference between surface returns for rain-filled ($S_R$) and rain-free ($S_0$) radar beams is due to rain attenuation:

$$R_m \approx (S_R - S_0) \cdot k(h_m/2) \cdot \beta \cdot (2h_m)^{-1} \quad (5)$$

The errors of this approach over water could be of an order of the uncertainties for the suggested here profiling method. The rain free ocean surface return ($S_0 \approx$ 35 dBZ) was obtained just prior entering the rain area at ~19:19:32 UTC (see Figure 3a). The agreement between the two CloudSat estimates is good over water but not over land where the surface reference method sometimes yields negative values of $R$ due to high and variable land returns. Note also that, unlike the suggested here attenuation-based profiling method, the ocean surface reference approach will not work for $R > 9$ mm h$^{-1}$, because heavier rains at the 8.2 km roundtrip interval will totally attenuate this return down to the CloudSat radar sensitivity limit of about −27 dBZ.

[20] Due to refraction and the Earth curvature, the center of the KLIX resolution volume (at a beam elevation of 1.7°) corresponds to heights of about 2.8 km (for the 83 km range) and 3.4 km (for the 102 km range). The NEXRAD radar beamwidth of about 1° and sampling strategy result in about 1.5 km (1 km) resolutions across (along) the beam. The resolution volumes with ground coordinates of their centers within ±0.5 km from the CloudSat ground track are used for comparisons. KLIX retrievals are somewhat larger than CloudSat retrievals using the method suggested here. KLIX rain rate estimates also exhibit more variability between neighboring points. Typical uncertainties of radar retrievals based on $Z - R$ relations (i.e., KLIX retrievals) can easily be as high as a factor of 2 and even greater. According to the data posted by the National Severe Storm Laboratory at http://www.nmq.nssl.noaa.gov, KLIX radar-based rain accumulations between 1900 and 2000 UTC on 31 July 2006 differed from surface gauge data located in the considered area (but not directly under the CloudSat track) by factors ranging from about 0.4 to 1.9 (depending on a gauge). This is in agreement with an estimate of a factor of 2 or even grater for NEXRAD rain rate uncertainties. Given these uncertainties, the CloudSat-NEXRAD comparisons cannot be regarded as a strict validation effort, but they are useful as a consistency check. Note also, that ground-based radars (e.g., NEXRAD) provide one of only few options for comparisons with CloudSat. Rain gauges typically provide accumulation amounts and cannot be effectively used for comparisons of instantaneous rain rates from CloudSat retrievals.

## 6. Concluding Remarks

[21] The results of this study indicate a possibility of rain rate profile retrievals from the CloudSat 94 GHz nadir-pointing radar using an attenuation-based method. Unlike the traditional radar methods that make use of estimates of non-attenuated reflectivity, this method takes advantage of the high attenuation in rain and low variability of non-attenuated reflectivities at W-band, and uses estimates of height derivatives of measured (attenuated) reflectivities. These estimates are then related to rain rates. The effective resolution of the proposed version of the method is 1.2 km, though rain rate retrievals could be available in a rain layer where CloudSat measurements are above noise except in the vicinity of the freezing level or surface because of echo contaminations by melting layer and ground returns. The method is immune to radar calibration errors and to signal attenuation in snow and melting layers. It provides vertical profiles and can be used regardless of the background (land/water) because the availability of surface returns is not required; however, it is consistent with the surface return approach for layer mean rain rates when such returns from water are available. Initial comparisons of the CloudSat attenuation-based retrievals with a weather service ground precipitation radar provided a general consistency check given uncertainties of the satellite and ground-based methods.

[22] The differential character of measurements of the suggested method makes it less susceptible to the effects of multiple scattering compared to traditional radar approaches. Nevertheless, future enhancements of this method should include corrections for multiple scattering. Extensive comparisons with other ground and satellite

methods are needed to better understand the scope of the applicability of the attenuation-based method.

[23] **Acknowledgments.** This study was supported by the CloudSat project.

## References

Battaglia, A., M. O. Ajewole, and C. Simmer (2005), Multiple scattering effects due to hydrometeors on precipitation radar systems, *Geophys. Res. Lett.*, *32*, L19801, doi:10.1029/2005GL023810.

Hitschfeld, W., and J. Bordan (1954), Errors inherent in the radar measurement of rainfall at attenuating wavelengths, *J. Meteorol.*, *11*, 58–67.

Iguchi, T., T. Kozu, R. Meneghini, J. Awaka, and K. Okamoto (2000), Rain-profiling algorithm for the TRMM precipitation radar, *J. Appl. Meteorol.*, *39*, 2038–2052.

L'Ecuyer, T. S., and G. L. Stephens (2002), An estimation-based precipitation retrieval algorithm for attenuating radars, *J. Appl. Meteorol.*, *41*, 272–285.

Matrosov, S. Y. (2005), Attenuation-based estimates of rainfall rates aloft with vertically-pointing $K_a$-band radars, *J. Atmos. Oceanic Technol.*, *22*, 43–54.

Matrosov, S. Y., T. Uttal, and D. A. Hazen (2004), Evaluation of radar reflectivity-based estimates of water content in stratiform marine clouds, *J. Appl. Meteorol.*, *43*, 405–419.

Matrosov, S. Y., P. T. May, and M. D. Shupe (2006), Rainfall profiling using Atmospheric Radiation Measurement program vertically pointing 8-mm wavelength radars, *J. Atmos. Oceanic Technol.*, *23*, 1478–1491.

Meneghini, R., T. Iguchi, T. Kozu, L. Liao, K. Okamoto, J. A. Jones, and J. Kwiatkowski (2000), Use of the surface reference techniques for path attenuation estimates from TRMM precipitation radar, *J. Appl. Meteorol.*, *39*, 2053–2070.

Stephens, G. L., and the CloudSat Science Team (2002), The CloudSat mission and the A-train. A new dimension of space-based observations of clouds and precipitation, *Bull. Am. Meteorol. Soc.*, *83*, 1771–1790.

S. Y. Matrosov, Cooperative Institute for Research in Environmental Sciences, University of Colorado and NOAA ESRL, 325 Broadway, Boulder, CO 80305, USA. (sergey.matrosov@noaa.gov)